CH9500741

LRP 530/95

October 1995

PARTIAL-DEPTH MODULATION STUDY OF ANIONS AND NEUTRALS IN LOW PRESSURE SILANE PLASMAS

C. Courteille, J.-L. Dorier, Ch. Hollenstein,
L. Sansonnens and A.A. Howling

C R P P

ÉCOLE POLYTECHNIQUE FÉDÉRALE DE LAUSANNE - SUISSE

VOL. № 04

LRP 530/95 October 1995

PARTIAL-DEPTH MODULATION STUDY OF ANIONS AND NEUTRALS IN LOW PRESSURE SILANE PLASMAS

C. Courteille, J.-L. Dorier, Ch. Hollenstein,
L. Sansonnens and A.A. Howling

Invited Paper
Presented at IUVSTA Workshop
Fuji-Yoshida, Japan, 20-22 September 1995
submitted to Plasma Sources Sci. Technol.

Partial-Depth Modulation Study of Anions and Neutrals in Low Pressure Silane Plasmas

C. Courteille, J.-L. Dorier, Ch. Hollenstein, L. Sansonnens and A. A. Howling

Centre de Recherches en Physique des Plasmas
Ecole Polytechnique Fédérale Lausanne,
Av. des Bains 21, CH-1007 Lausanne, Switzerland

Abstract. Partial-depth modulation of the rf power in a capacitive discharge is used to investigate the relative importance of negative ions and neutral radicals for particle formation in low power, low pressure silane plasmas. For less than 85% modulation depth, anions are trapped indefinitely in the plasma and particle formation ensues, whereas the polymerised neutral flux magnitudes and dynamics are independent of the modulation depth and the powder formation. These observations suggest that negative ions could be the particle precursors in plasma conditions where powder appears many seconds after plasma ignition. Microwave interferometry and mass spectrometry were combined to infer an anion density of ~ 7.10^9 cm^{-3} which is approximately twice the free electron density in these modulated plasmas.

1. Introduction

The origin of particulate contamination [1-4] during plasma processing may depend on precursors which are neutral, charged (positive or negative), or any combination of these, according to the gas types and plasma conditions employed. The authors have discussed various aspects of particle formation in recent publications [5-8] with regard to low power, low pressure silane rf plasmas in which particles appear only after many seconds - these conditions are appropriate for the deposition of high quality amorphous silicon material.

This paper concentrates specifically on partial-depth power modulation experiments [9] which are intended to discriminate between the rôles of anions and neutrals in particle formation for the plasma conditions stated above. The principle is that negative ions can escape during the afterglow of ON/OFF-modulated plasmas but remain confined by the sheath of a weak afterglow plasma during partial-depth power modulation; neutrals, on the other hand, can diffuse from the discharge at all times and their rate of production is similar for both modulation conditions provided that the rf power in the weak afterglow plasma is small compared to the principal plasma period. Microwave interferometry and mass spectrometry are combined to provide an estimate of anion density inferred from the time dependence of the electron and positive ion densities during a modulation cycle.

2. Experimental apparatus

The experimental apparatus [5] shown in Fig. 1 is a conventional parallel-plate rf capacitive reactor comprising two 13-cm-diam electrodes with a 2.5 cm electrode gap and a grounded guard screen on the lower, rf electrode. The gas inlet is in the side wall of the cubic grounded vacuum chamber of side 40 cm. For all experiments reported here the silane flow rate was 30 sccm with pumping speed control to maintain 0.1 mbar pressure. The formation of powder suspended in

the plasma was qualitatively monitored by measuring the extinction of a 10 mW He-Ne laser beam traversing the plasma along the electrode diameter.

The lower electrode was connected via a π matching box and rf power-meter to a wideband, capacitively-coupled rf amplifier. The 10 MHz excitation frequency sinewave was amplitude-modulated at 1 kHz as described in previous work [5]. The electrode voltage waveform was measured directly at the underside of the rf electrode with a passive probe and 1 GHz oscilloscope which were integral components of the reactor and so introduced no perturbation to the system impedance. The rise- and fall-time of the electrode voltage in vacuum was less than a microsecond. The specific plasma parameters and rf power waveform used are referenced in each figure caption.

8.3 GHz single-pass microwave interferometry, using a standard technique [10], provided time-resolved measurements (overall response time < 3 μs) of the free electron absolute density, spatially-averaged over the electrode gap (see Fig. 1) with a sensitivity better than 10^8 electrons/cm^3. The microwave diode signals were calibrated using a phase-shifter and acquired by a 1 GHz digital oscilloscope averaging over 20 acquisitions. Spurious reflections within the vacuum chamber were suppressed by placing glass ceramic ('Macor') blocks between the electrodes and the walls.

The Hiden Analytical Limited Plasma Monitor [11] type HAL-EQP 500 is equipped for neutral analysis, ion extraction, mass and energy measurements. Single-stage differential pumping maintained a spectrometer operating pressure of < 6.10^{-6} mbar for 0.1 mbar silane pressure in the reactor. Negative ions were measured up to the monitor mass limit of 512 amu with the monitor mounted either in the ground electrode (Fig. 1) or to the side of the electrode gap [5]. The important question of non-perturbative anionic cluster sampling has been considered elsewhere [5,8]. Ions entered the monitor first through a 5-mm-diam orifice in the grounded spectrometer head and then a 0.1 mm aperture in the biased extractor electrode. A +40 V (-50 V) bias was used for negative (positive

ions) respectively. Acceleration into a drift tube was followed by a 45 degree sector electrostatic analyser to select the transmitted ion energy before the quadrupole mass filter and channeltron detector. For time-resolved measurements, the channeltron pulses were counted cumulatively over 1000 modulation cycles by a multi-channel scalar triggered synchronously with the amplitude modulation signal [5]. The 5 μs time resolution was fixed by the scalar dwell time. The transit time of an ion crossing the spectrometer introduces a non-negligible (> 100 μs) mass-dependent instrumental delay with respect to the power modulation timing - these transit times were calibrated [5] and implicitly subtracted from all the time-resolved data presented here.

3. Results and discussion

3.1 Partial-depth modulation

The principle of the partial-depth modulation experiment [9] is that the sheath does not collapse and anions cannot escape unless the modulation depth of the rf voltage exceeds ~ 85%. The results of our experiment are as follows: In Fig. 2(a), with ON/OFF power modulation (corresponding to 100% modulation depth), a negative ion flux was measured during the afterglow but no powder was detectable - this is the situation as described previously [5,6,12]. After 4.5 minutes without powder formation, the rf voltage during the afterglow was set at 48 V (Fig. 2(b)), whereupon the sheath no longer fully collapsed: The anion flux abruptly disappeared and powder appeared after 40 s. The principle of the experiment is that the magnitudes and dynamics of neutral species production and loss rates are essentially unchanged by going from Fig. 2(a) to 2(b) since neutrals are not affected by the sheaths (the time-averaged rf power increases by only ~ $(V_{ag}/V_{pl})^2 = (0.15)^2 < 3\%$), whereas the anion flux is switched on or off. The partial-depth modulation technique therefore discriminates between neutrals and anions, and the interpretation is that negative ions are precursors to particle growth in these low pressure silane plasmas [5,6,8,12].

Note that the plasma/afterglow durations must be chosen according to the plasma parameters in conjunction with anion measurements: If the afterglow period is too short (for example, at 10 kHz modulation frequency [5,6,12]), the sheath potentials do not fully collapse and anions remain trapped even for complete ON/OFF power modulation. Equivalently, if the plasma period is so long as to result in strong polymerisation during a single plasma period, particles may form independently of the modulation depth used. The results in these two cases would consequently be meaningless if interpreted in terms of anions.

The transition in anion flux in passing from Fig. 2(a) to (b) is shown in more detail in Fig. 3. When the modulation depth is larger than 90 % (V_{ag}/V_{pl} < 40 V/400 V), the anions escape (see Fig. 2(a) and Ref. 5) and for modulation depths less than 85 % (V_{ag}/V_{pl} > 60 V/400 V), the anions remain trapped [9]. On closer inspection we find a narrow 'bistable' régime which shows that the transition is not simply a threshold effect: If V_{ag} is increased gradually starting from zero (V_{pl} constant) up to 60 V, an instantaneous transition occurs (without changing the external parameters) whereupon V_{ag} drops to 40 V and the anion flux abruptly disappears. Conversely, if V_{ag} is initially higher than 60 V, it can be reduced to 40 V before a switch to 60 V occurs and the anion flux appears. These two cases are represented schematically by the ABCD and FEDC trajectory in Fig. 3 which is highly reproducible. Within the transition zone, the plasma can remain indefinitely in either of the two states B-C or E-D for the same V_{ag} value, but there is no stationary state corresponding to segment C-D.

The two sets of measurements in the left- and right-hand columns of Fig. 4 were both made for V_{ag} = 55 V (within the transition zone), where the sheath potential reverses for the left column but not for the right column. The different diagnostics are described in turn:

In the left-hand side of Fig. 4(a) and (b), the high- and low-energy components of the positive ion flux, and the electron density all fall to zero in ~ 50 μs; the negative ion flux then appears and decays during the afterglow period

- this is the usual situation [5,9] in an ON/OFF-modulated plasma. For the partial-depth modulation on the right-hand side of Fig. 4, the discharge sheath potential drops sharply to a low value, but not to zero. Therefore, the low energy component of the positive ion flux persists during the weak afterglow period, although the electron density falls to below the detection limit of the interferometer (a residual density of electrons must persist in order that the electropositive sheaths are maintained). To preserve quasi-neutrality, we infer that the remaining positive ion density is balanced by the trapped negative ion density. For these partial-depth modulation conditions of the right-hand column where the negative ions are retained, a fine powder suspended in the plasma eventually formed after 1 minute (as observed by laser scattering) - this is consistent with the experiment described in Fig. 2. The peak-to-peak envelope of the voltage applied to the rf electrode is shown in Fig. 4(c). The rf voltage is shifted negatively during the full-power period by the strong self-bias due to the asymmetry of the electrode effective areas [13]. The minor differences between the waveforms with and without powder in Fig. 4(c) were a highly reproducible and reliable indicator of the transition between segments B-C and D-E in Fig. 3. Note that the voltage amplitudes during the plasma V_{pl} and afterglow V_{ag} have the same values in both cases as discussed regarding the transition zone of Fig. 3.

3.2 Dynamics of the neutral flux.

Fig. 4(b) also shows the measured flux of disilicon neutrals (Si_2H_x), ionised by a 20 eV electron beam just behind the extraction orifice of the mass spectrometer. This signal was measured using the same time resolution as for the positive and negative ions. Monosilicon neutrals (SiH_x) were not monitored here because appearance mass spectrometry [14] is necessary to distinguish between radicals produced from silane cracking and radicals formed in the plasma itself. In contrast, the background signal from the higher silanes without plasma was

negligible and so these signals were reliable indicators of the polymerised neutrals produced by the plasma.

The mass spectrum and flux of polysilicon neutrals were unchanged between the two columns in Fig. 4(b), ie the neutrals were unaltered in the presence or absence of powder formation. It is also significant that the flux of neutrals undergoes no variation during a modulation cycle. Therefore, any neutral polymerisation pathway to particle formation [15] would not be affected by kHz power modulation [5,6,12] even if the monosilicon radical reaction times were sub-millisecond, because the intermediate polysilicon neutral species, which are the next steps in a neutral polymerisation scheme, do not react or diffuse on a sufficiently-short timescale in these low power, low pressure silane plasmas.

Finally, the negative ion loss flux is anti-correlated with powder formation [6,8,12], whether controlled by modulation frequency [12] or modulation depth [8] (Fig. 2). To summarise, the above data and interpretation suggest that negative ions are involved in powder formation for these plasma conditions in which particles appear slowly, many seconds after plasma ignition.

3.3 Estimation of the negative ion density

The anion density cannot be directly measured during the plasma with the diagnostics described above; other measurements by Shiratani *et al* [16] and Tochikubo *et al* [17] have previously shown significant densities of anions in continuous silane plasmas. In the experiments described below, the free electron absolute density n_e is measured by microwave interferometry and so if the positive ion density n^+ can be measured and calibrated using the mass spectrometer, the anion density n^- is given by the difference: $n^- = n^+ - ne$, provided that the amount of electron charges on particles can be neglected or accounted for.

From previous work [5,18] it is known that the monosilicon hydride cations, SiH_x^+, represent the majority of the positive ion flux. By using a

degraded mass resolution, the temporal behaviour of the several monosilicon radicals (SiH_x^+) could be monitored simultaneously. To determine the cation density as a function of time, it is necessary to follow the time evolution of the ion energy distribution; this was achieved by changing the mass spectrometer energy analyser value in steps of 2 V (equal to the instrumental energy resolution) and acquiring the flux intensity variation during the modulation cycle. The time-development of the energy spectrum is shown in Fig. 5 for the partial-depth modulation case of V_{pl} = 400 V and V_{ag} = 60 V. The corresponding ion energy maxima are 40 eV and 20 eV respectively, equal to the time-averaged plasma potential given approximately by [13] $(V_{pl} + V_{sb})/2$ for capacitive sheaths (the large self-bias V_{sb} = 310 V during the plasma period in Fig. 4(c) is responsible for the relatively low ion energy at the grounded electrode). It was verified that the sum of the obtained energy spectra over one cycle corresponded to the form of the time-averaged energy spectrum measured directly with an acquisition dwell time much longer than the modulation period.

The positive ion density time-dependence was estimated from $n^+ \propto \int \Gamma(\varepsilon_i)/\sqrt{\varepsilon_i}\ d\varepsilon_i$, where it is assumed that the global cation density is approximately proportional to the cation flux $\Gamma(\varepsilon_i)$ measured at the electrode. This positive ion density is compared to the measured free electron density in Figure 6. Note that the positive ion density does not fall to zero whereas the electron density falls below the limit of detection - as discussed in Section 3.1, we infer that the remaining positive ion density is balanced by the trapped negative ion density. In order to calibrate the positive ion density, we make use of the similar dynamic behaviour of the electron density signal: When the rf voltage amplitude switches from 400 V to 60 V at t = 0.5 ms, both the cation and electron densities fall abruptly in ~50 μs. We attribute these losses to rapid ambipolar diffusion of electrons and positive ions to the electrodes as the sheath potentials and dc self-bias drop sharply on a similar timescale as shown in Fig. 4(c); the high-mobility, energetic electrons escape rather than the heavy negative

ions which maintain charge-neutrality with the remaining positive ions in the plasma volume, thus permitting the electron density to decay without the appearance of large electric fields. Other loss processes, such as electron-ion dissociative recombination (time constant [19] ~ $10^{-7}/\sqrt{T_e}$ cm^3 s^{-1}, with T_e ~ 2 - 3 eV) are at least an order of magnitude too slow to account for this rapid loss. Note also that electron loss purely by attachment to neutrals would not explain the simultaneous fall in positive ion density. The positive ion signal is thus calibrated by equating the simultaneous drop in positive ion and electron densities.

The time-dependent negative ion density is finally given by the difference between the positive ion and electron densities in Fig. 6 : we infer a total anion density of ~ 7.10^9 cm^{-3} which is approximately double the free electron density in these modulated, pure silane plasmas. This is not unreasonable since plasmas in electronegative gases, such as halogens, can contain an order of magnitude more anions than electrons [22]. Other estimates have been made by different authors in silane-containing plasmas [17,19,20]: Shiratani *et al* [16] estimate ~ 10^9 cm^{-3} even for silane diluted to below 1% in helium, and a fluid code [21] yields n^-/n_e ~10^1 for the same plasma parameters as the present work. In Fig. 6, after the electron density has mostly disappeared, the ion density gradually decays away by diffusion and/or by mutual neutralisation. Taking the coefficient of mutual neutralisation [19] to be 5.10^{-7} cm^3 s^{-1}, the ion densities would fall to half their value in ~ 0.3 ms showing that mutual neutralisation is likely to contribute to ion losses in the weak afterglow.

4. Conclusions

Partial-depth rf power modulation of low power, low pressure silane plasmas has been used to investigate the importance of negative ions and neutrals in the formation of particulate contamination. The level of rf voltage in the afterglow period determines whether the negative ions remain trapped, or are de-trapped

from the discharge. Powder forms when the negative ions are trapped but is absent otherwise, whereas the neutrals' mass spectrum, flux, and time-dependence are unchanged by the rf voltage level. This indicates the rôle of negative ions as particle precursors in these plasmas with slow particle formation. Finally, the negative ion density is estimated to be approximately twice the electron density in these power-modulated plasmas.

Acknowledgments

This work was funded by Swiss Federal Research Grants BBW 93.0136 (for Brite-Euram project BE-7328) and BEW 9400051.

References

[1] Selwyn G S 1994 *Plasma Sources Sci. Technol. 3, 340*

[2] Garscadden A, Ganguly B N, Haaland P D and Williams J 1994 *Plasma Sources Sci. Technol. 3, 239*

[3] Perrin J, Böhm Ch, Etemadi R and Lloret A 1994 *Plasma Sources Sci. Technol. 3, 252*

[4] Veprek S, Schopper K, Ambacher O, Rieger W and Veprek-Heijman M G J 1993 *J. Electrochem. Soc. 140, 1935*

[5] Howling A A, Sansonnens L, Dorier J-L and Hollenstein Ch 1994 *J. Appl. Phys. 75, 1340*

[6] Hollenstein Ch, Dorier J-L, Dutta J, Sansonnens L and Howling A A 1994 *Plasma Sources Sci. Technol. 3, 278*

[7] Dorier J-L, Hollenstein CH and Howling A A 1995 *J. Vac. Sci. Technol. A. 13, 918*

[8] Howling A A, Courteille C, Dorier J-L, Sansonnens L and Hollenstein Ch *submitted to Pure & Applied Chemistry*

[9] Overzet L J, Beberman J H and Verdeyen J T 1989 *J. Appl. Phys. 66, 1622*

[10] Meuth H and Sevillano E *Plasma Diagnostics* Volume 1 ed. O. Auciello and D. L. Flamm (Academic Press) pp 239.

[11] Hiden Analytical Limited, Gemini Business Park, Warrington WA5 5TN, UK.

[12] Howling A A, Dorier J-L and Hollenstein Ch 1993 *Appl. Phys. Lett. 62, 1341*

[13] Köhler K, Coburn J W, Horne D E, Kay E and Keller J H 1985 *J. Appl. Phys. 57, 59*

[14] Kae-Nune P, Perrin J, Guillon J, and Jolly J 1995 *Plasma Sources Sci. Technol. 4, 250*

[15] Watanabe Y, Shiratani M and Makino H 1990 *Appl. Phys. Lett. 57, 1616*

[16] Shiratani M, Fukuzawa T, Eto K and Watanabe Y 1992 *Jpn. J. Appl. Phys. 31, L1791*

[17] Tochikubo F, Suzuki A, Kakuta S, Terazono Y and Makabe T 1990 *J. Appl. Phys. 68, 5532*

[18] Haller I 1980 *Appl. Phys. Lett. 37, 282*

[19] Kushner M J 1988 *J. Appl. Phys. 63, 2532*

[20] Overzet L J and Verdeyen J T 1986 *Appl. Phys. Lett. 48, 695*

[21] Boeuf J-P and L. C. Pitchford L C 1995 *Phys. Rev. E 51, 1376*; and Kinema Research Associates SIGLO-RF (Simulation of Glow discharges RF excited, capacitively-coupled) modeling software.

[22] Haverlag M, Kono A, D. Passchier D, Kroesen G M W, W. J. Goedheer and de Hoog F J 1991 *J. Appl. Phys. 70, 3472*

Figure Captions

Figure 1: Schematic of the plasma reactor, microwave interferometer waveguides, and the differentially-pumped Hiden mass spectrometer mounted in the ground electrode.

Figure 2: Partial-depth modulation experiment. Powder was monitored by the extinction of a He-Ne laser beam. The disilicon anion flux [5] in (a) was measured with the Hiden monitor and a multi-channel scalar.The initial rf voltage amplitude modulation is shown in inset (a). Arrows mark the time when the afterglow voltage was increased to 48 V (inset (b)). Electrode temperature 66 °C, 0.1 mbar silane and 10 MHz rf frequency; the time-averaged rf power for both (a) and (b) was 10 W.

Figure 3: Dependence of the trisilicon anion loss flux on modulation depth: For a fixed rf voltage of V_{pl} = 400 V during the plasma period, the anion signal was monitored as a function of the rf amplitude V_{ag} during the 'afterglow' period. See text for description. Plasma parameters as for Fig. 2

Figure 4: Left-hand column: (a) Positive and negative ion fluxes, (b) electron density and neutral flux, and (c) electrode rf voltage envelope, each as a function of time during a 1 kHz power modulation cycle. The modulation depth is 86.3% (V_{ag}/V_{pl} = 55 V/400 V) and no powder was observed. Right-hand column: the same measurements with the same modulation voltages, but with powder formation. The plasma conditions for the left- and right-hand columns correspond to the bistable states in the transition zone of Fig. 3, as can be seen by comparing the difference in negative ion fluxes in (a). Plasma parameters as for Figs. 2 and 3.

Figure 5: The measured time development of the monosilicon positive ion flux energy distribution during a single cycle of 1 kHz partial-depth power modulation. The maximum ion energy collapses from 40 eV to 20 eV after 500 μs. Plasma conditions as for the right-hand column in Fig. 4.

Figure 6: Electron density, measured by microwave interferometry, and monosilicon positive ion density, estimated from integration over the flux energy distribution in Fig. 5, during a cycle of 1 kHz partial-depth power modulation. The negative ion density was deduced by the requirement of quasi-neutrality: The negative and positive ion densities therefore almost coincide when the electron density falls below the detection limit of the interferometer. Plasma conditions as for the right-hand column in Fig. 4.

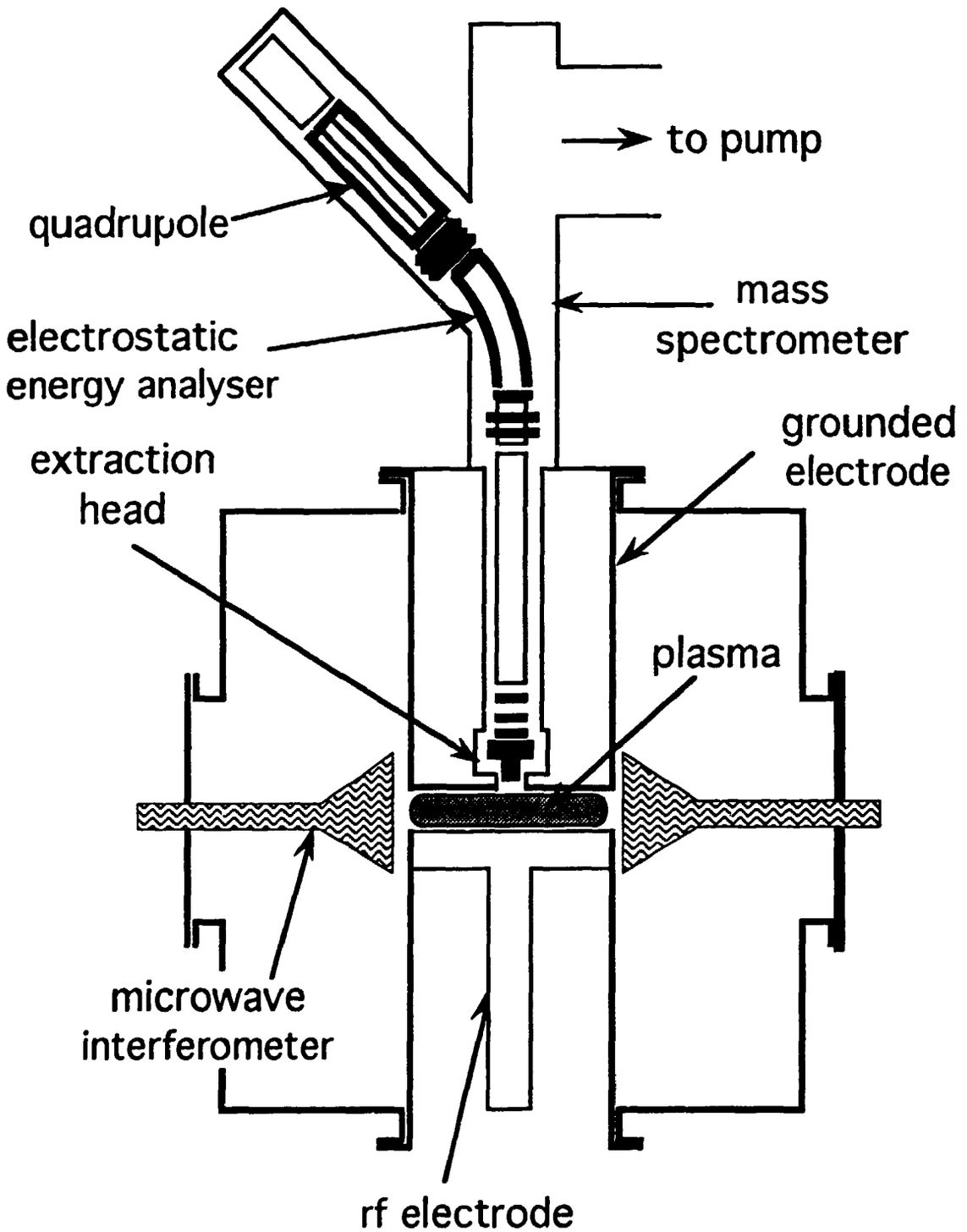
to pump
quadrupole
mass
spectrometer
electrostatic
energy analyser
grounded
electrode
extraction
head
plasma
microwave
interferometer
rf electrode

Fig. 1

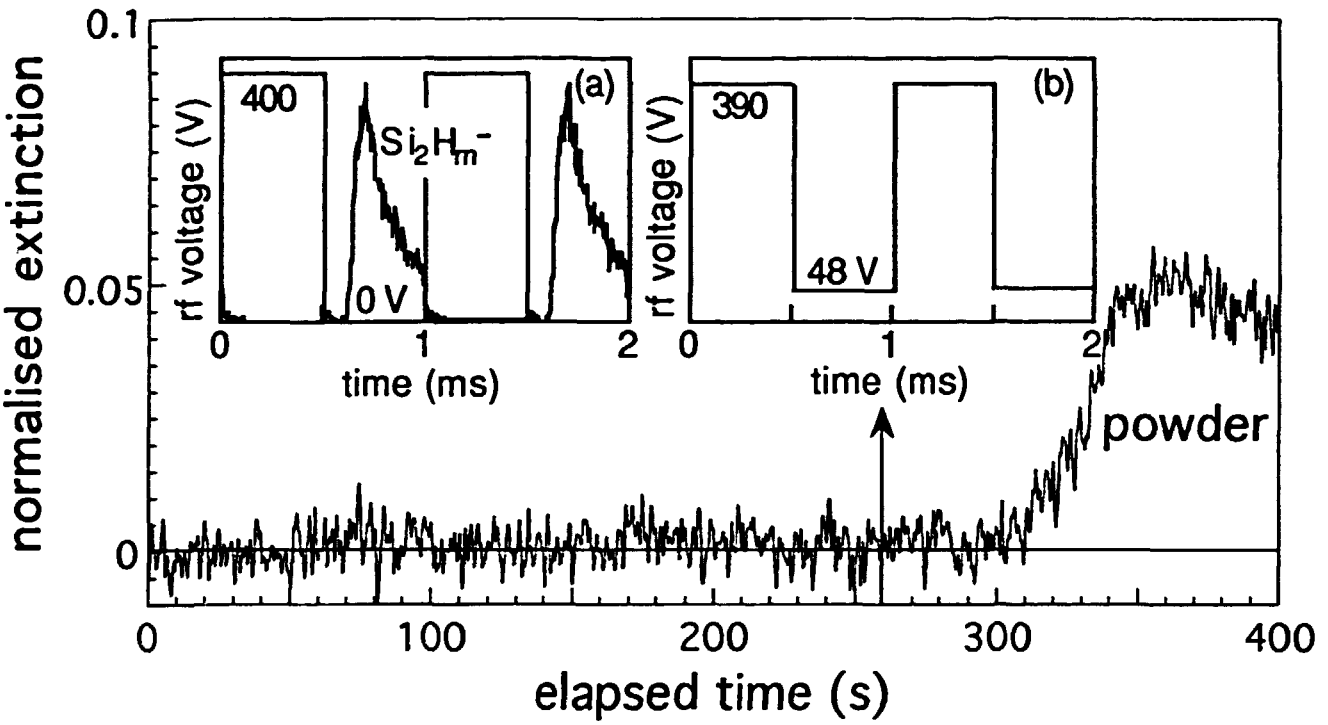
0.1
0.05
0
normalised extinction
400
0 V
(a)
$Si_2H_m^-$
rf voltage (V)
0
1
2
time (ms)
390
48 V
(b)
rf voltage (V)
0
1
2
time (ms)
powder
0
100
200
300
400
elapsed time (s)

Fig. 2

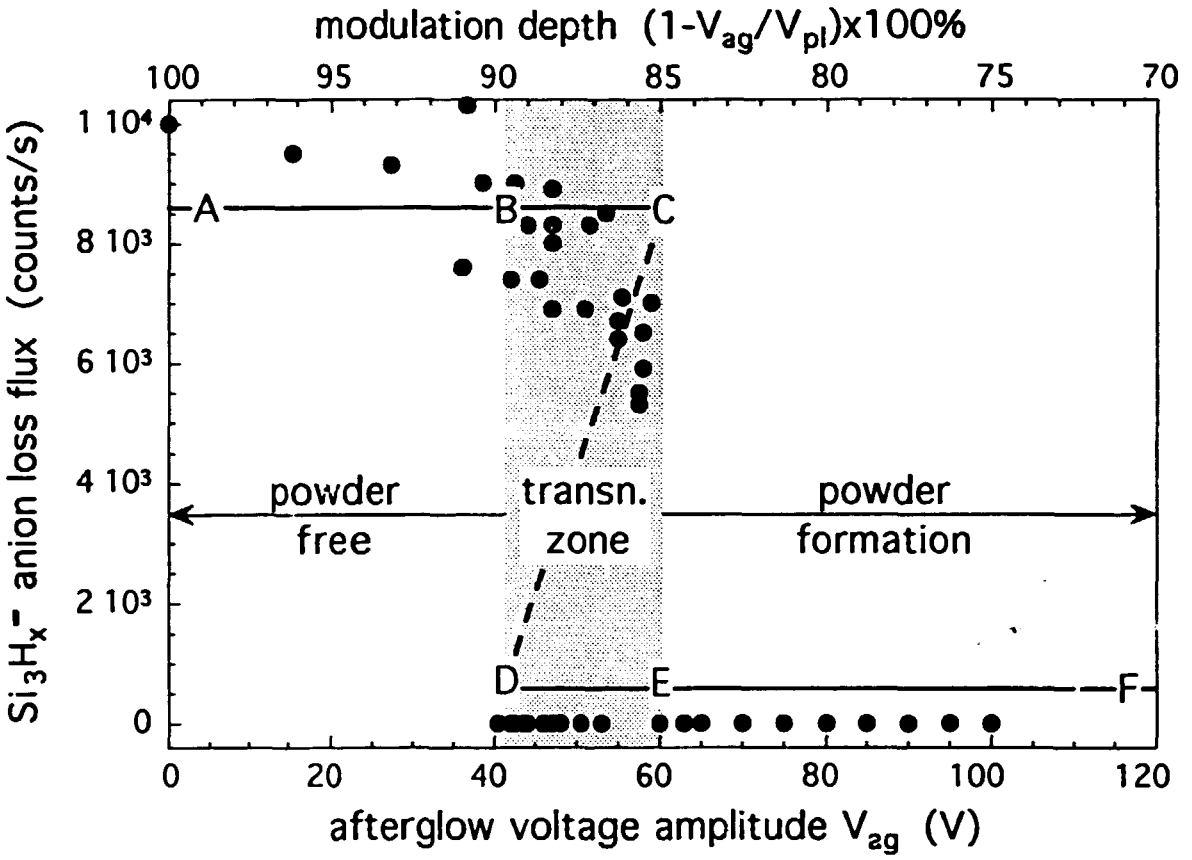
modulation depth (1-V_{ag}/V_{pl})x100%
100
95
90
85
80
75
70
1 10⁴
8 10³
6 10³
4 10³
2 10³
0
$Si_3H_x^-$ anion loss flux (counts/s)
A
B
C
D
E
F
powder free
transn. zone
powder formation
0
20
40
60
80
100
120
afterglow voltage amplitude V_{ag} (V)

Fig. 3

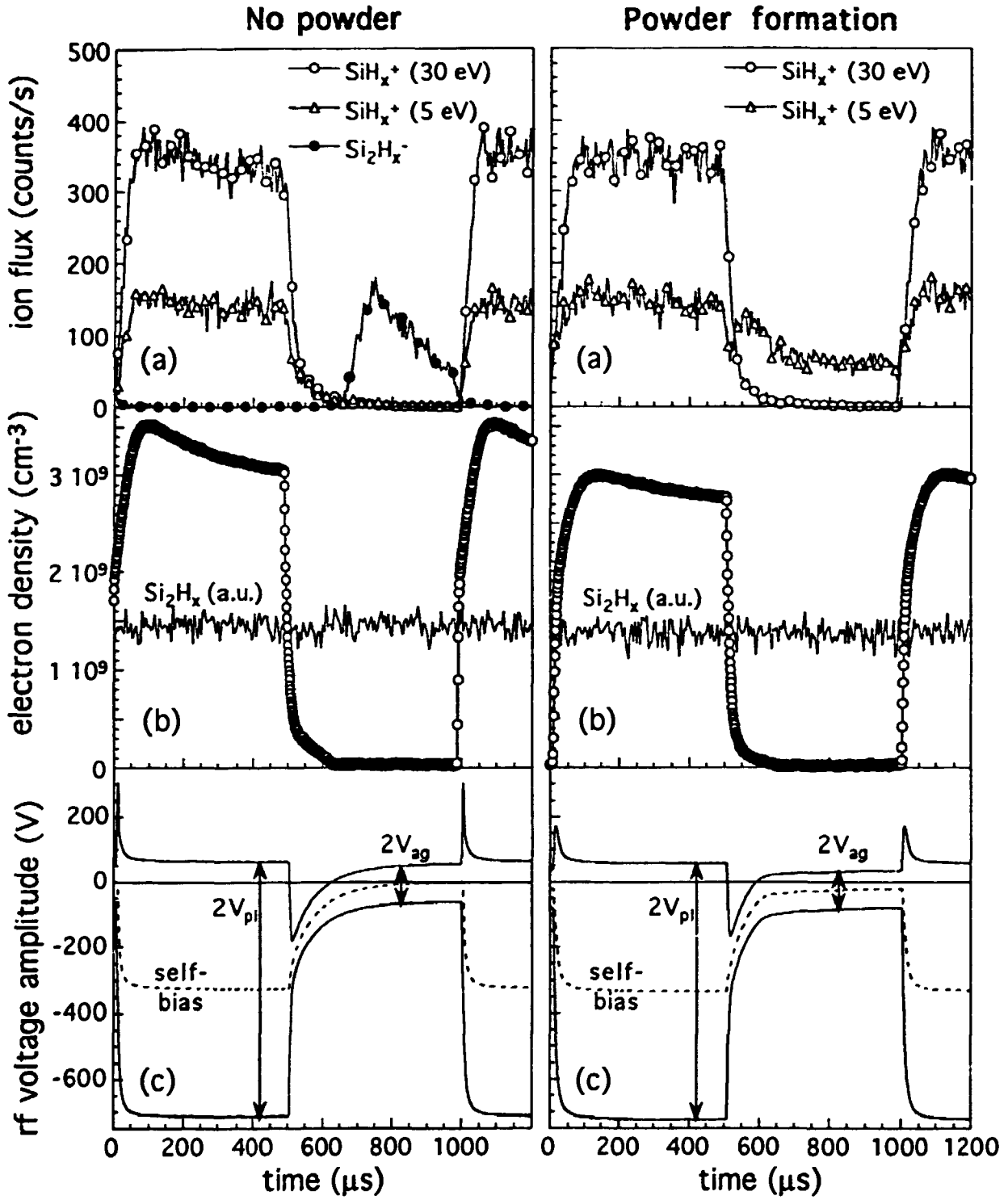
No powder
Powder formation
ion flux (counts/s)
SiHx+ (30 eV)
SiHx+ (5 eV)
Si2Hx-
(a)
electron density (cm-3)
Si2Hx (a.u.)
(b)
rf voltage amplitude (V)
2Vag
2Vpl
self-bias
(c)
time (μs)

Fig. 4

Fig. 5

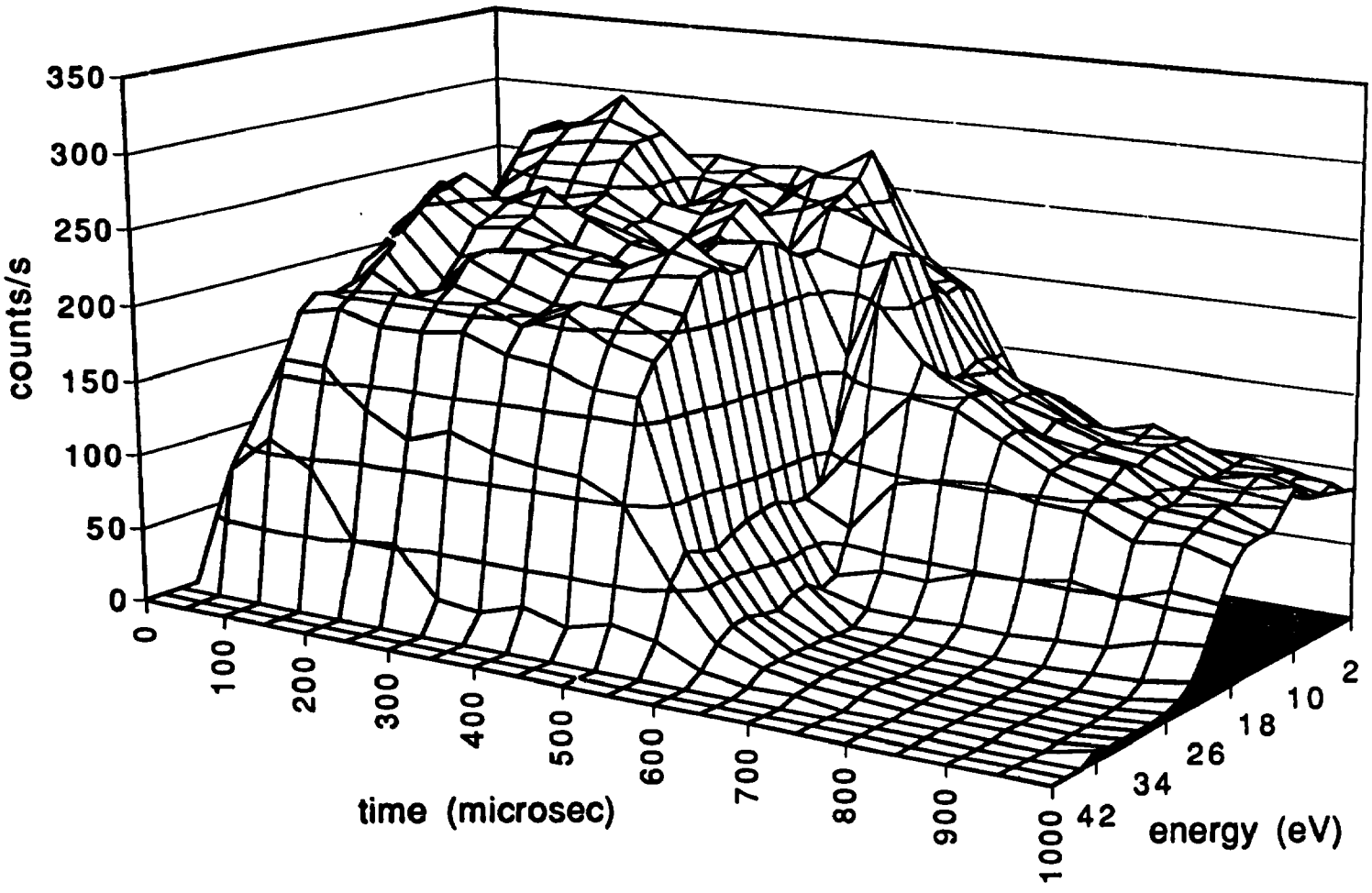
counts/s
350
300
250
200
150
100
50
0
0
100
200
300
400
500
600
700
800
900
1000
time (microsec)
42
34
26
18
10
2
energy (eV)

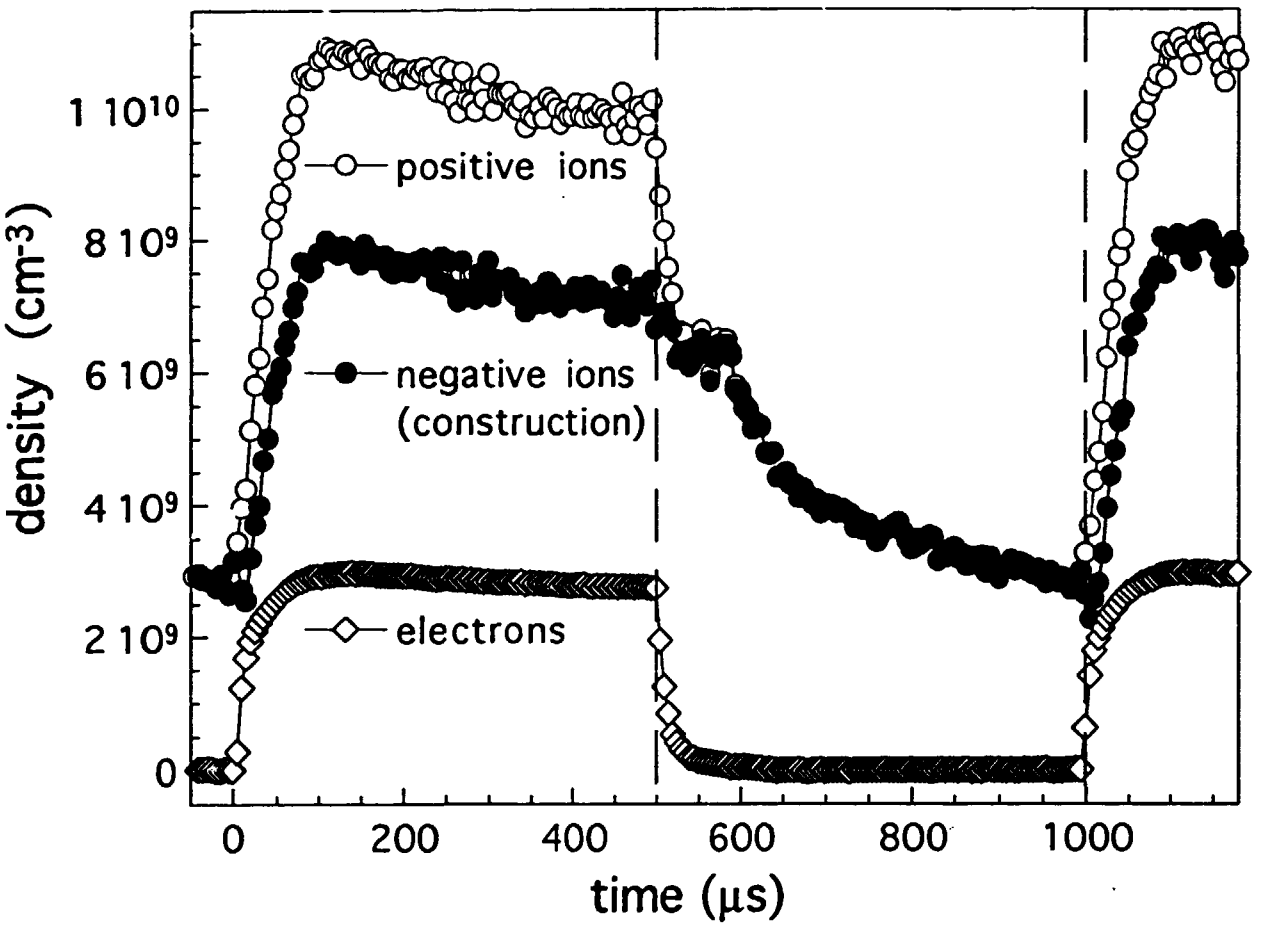
1 10¹⁰
8 10⁹
6 10⁹
4 10⁹
2 10⁹
0
density (cm⁻³)
positive ions
negative ions
(construction)
electrons
0
200
400
600
800
1000
time (μs)

Fig. 6